Received: 26 January 2022 | Accepted: 19 August 2022

DOI: 10.1111/gcb.16431

Global Change Biology WILEY

RESEARCH ARTICLE

Evidence for evolutionary adaptation of mixotrophic nanoflagellates to warmer temperatures

Michelle Lepori-Bui[1,2] | Christopher Paight[1] | Ean Eberhard[1] | Conner M. Mertz[1,3] | Holly V. Moeller[1]

[1]Department of Ecology, Evolution, and Marine Biology, University of California – Santa Barbara, Santa Barbara, California, USA

[2]Washington Sea Grant, University of Washington, Seattle, Washington, USA

[3]Department of Biology, University of New Mexico, Albuquerque, New Mexico, USA

Correspondence
Michelle Lepori-Bui, Washington Sea Grant, University of Washington, 3716 Brooklyn Ave NE, Seattle, WA 98105, USA.
Email: mleporibui@ucsb.edu

Funding information
National Science Foundation, Grant/Award Number: NSF-OCE 185119

Abstract

Mixotrophs, organisms that combine photosynthesis and heterotrophy to gain energy, play an important role in global biogeochemical cycles. Metabolic theory predicts that mixotrophs will become more heterotrophic with rising temperatures, potentially creating a positive feedback loop that accelerates carbon dioxide accumulation in the atmosphere. Studies testing this theory have focused on phenotypically plastic (short-term, non-evolutionary) thermal responses of mixotrophs. However, as small organisms with short generation times and large population sizes, mixotrophs may rapidly evolve in response to climate change. Here, we present data from a 3-year experiment quantifying the evolutionary response of two mixotrophic nanoflagellates to temperature. We found evidence for adaptive evolution (increased growth rates in evolved relative to acclimated lineages) in the obligately phototrophic strain, but not in the facultative phototroph. All lineages showed trends of increased carbon use efficiency, flattening of thermal reaction norms, and a return to homeostatic gene expression. Generally, mixotrophs evolved reduced photosynthesis and higher grazing with increased temperatures, suggesting that evolution may act to exacerbate mixotrophs' effects on global carbon cycling.

KEYWORDS
carbon use efficiency, experimental evolution, metabolism, *Ochromonas*, thermal reaction norms

1 | INTRODUCTION

Mixotrophs, organisms that use a combination of autotrophy and heterotrophy to gain energy and nutrients, are increasingly recognized as omnipresent members of planktonic food webs and regulators of global biogeochemical cycles (Caron, 2016; Mitra et al., 2014; Ward & Follows, 2016; Worden et al., 2015). "Constitutive mixotrophs" are chloroplast-bearing protists that have retained the ability to eat (Mitra et al., 2016; Stoecker, 1998). These mixotrophs occur on a spectrum of metabolic strategies, ranging from primarily phototrophic (feeding when nutrients needed for photosynthesis are limiting) to primarily heterotrophic (photosynthesizing when prey are limiting) (Stoecker, 1998). Though different species of mixotrophs may favor one mode of carbon acquisition over the other in ideal conditions, the balance between autotrophy and heterotrophy is also affected by environmental factors including temperature, light and prey availability.

As a result of their flexible metabolism, mixotrophs may act as either carbon sources or sinks. For example, mixotrophs are

predicted to contribute substantially to primary production in mature ecosystems (Mitra et al., 2014), and they can account for over 80% of total chlorophyll in the open ocean (Zubkov & Tarran, 2008). They have also been found to drive carbon remineralization as the dominant grazers in oligotrophic gyres (Hartmann et al., 2012). Ocean ecosystem models predict that incorporating mixotrophy can promote the accumulation of biomass in larger size classes, increasing estimates of carbon export via the biological carbon pump by 60% (Ward & Follows, 2016). However, accurate model predictions require a better understanding of mixotroph metabolic flexibility, particularly in the face of ocean warming.

Rising ocean temperatures due to climate change will fundamentally affect oceanic ecosystems by altering the metabolic functions of marine organisms (Gillooly et al., 2001). According to the metabolic theory of ecology, metabolic rates increase exponentially with temperature (Brown et al., 2004). Because heterotrophic processes are more sensitive to temperature increases than photosynthetic processes (Allen et al., 2005; Rose & Caron, 2007), mixotrophs are predicted to become more heterotrophic at higher temperatures (Allen et al., 2005; Wilken et al., 2013), increasing their emission of carbon dioxide. Further, mixotrophs are dominant in the low-nutrient stratified water of subtropical gyres (Hartmann et al., 2012; Mitra et al., 2016), which are expected to expand with climate change (Polovina et al., 2008). Rising temperatures are also associated with decreases in body size (Gillooly et al., 2001; Malerba & Marshall, 2020), which reduces sinking rates, leading to cascading effects to carbon export by the biological carbon pump. Together, these changes could increase carbon dioxide accumulation in the atmosphere, generating a positive feedback loop.

Relatively few studies have tested the hypothesis that mixotrophs will become more heterotrophic with increased temperatures. Wilken et al. (2013) found a shift towards heterotrophy at higher temperatures in a primarily phagotrophic freshwater mixotroph, *Ochromonas* sp., after 2–4 weeks of acclimation to new temperatures. Conversely, Princiotta et al. (2016) found the opposite effect after 5 days of thermal acclimation in an obligately phototrophic freshwater mixotroph, *Dinobryon sociale*. These contrasting results show that predicting mixotrophs' response to increased temperature is complicated by many factors, including the diversity of mixotrophic organisms and how they balance their metabolism. Furthermore, due to the short timescale of these experiments (between 5 days and 4 weeks for slower-growing organisms), these results represent the organism's phenotypic plasticity, defined as the ability of a single genotype to exhibit different traits as a function of abiotic conditions. Such phenotypically plastic responses are expected to be reversible, and to not have arisen due to heritable genetic change. However, due to their short generation times, fast growth rates and large population sizes, microbes may rapidly adapt (via heritable evolutionary changes in genotype) to changing conditions. For example, a growing body of evolutionary experiments has shown that some phytoplankton are capable of adaptive evolution within several hundred generations (Barton et al., 2020; Listmann et al., 2016; O'Donnell et al., 2018; Padfield et al., 2016; Schaum et al., 2018). In some cases, these adaptations reversed short-term responses to increasing temperature, such as through the reduction of respiratory costs (Barton et al., 2020; Padfield et al., 2016). Although high taxonomic diversity mean lineages likely vary in their responses (Collins et al., 2014), to our knowledge, no mixotrophs have been similarly experimentally evolved.

Here, we quantified the evolutionary responses of mixotrophs to temperature change and related these responses to mixotrophic contributions to carbon cycling in the oceans. Specifically, we asked: Do mixotrophs adapt to different temperatures? What changes can be observed in carbon cycle-relevant traits when comparing their plastic and evolved responses? And what are some of the potential mechanisms for adaptation? We experimentally evolved two related strains of mixotrophic nanoflagellates—one obligate phototroph, requiring light but with increased growth rate with the presence of prey, and one facultative phototroph, requiring prey but able to grow in darkness—to different temperature treatments for 3 years (between 400 and 700 generations, depending on evolutionary temperature), to quantify adaptation. We varied light availability to manipulate selection for photosynthesis, and measured carbon cycle-relevant traits including metabolic rates (photosynthesis, grazing, and respiration), photosynthetic parameters (pigment content and photosynthetic efficiency), and cell size. We found evidence for adaptive evolution to both hot and cold temperatures in the obligately phototrophic strain, but only under high light conditions. Although differences in fitness over time were more variable in the facultative phototroph, evolution increased carbon use efficiency and reversed some of the short-term stress responses of control lineages. All lineages showed evolved responses in carbon cycle-relevant traits at the end of our experiment that could exacerbate mixotroph contributions to climate change.

2 | MATERIALS AND METHODS

2.1 | Mixotroph cultures and maintenance

We experimentally evolved two marine lineages from the genus *Ochromonas*, a widely distributed group of mixotrophic nanoflagellates. These cultures, purchased from the National Center for Marine Algae and Microbiota (NCMA, Bigelow Laboratory), represent different degrees of metabolic flexibility: Strain CCMP 1391 is obligately phototrophic (requiring light to survive, but has increased growth rate with the presence of prey) (Moeller et al., 2019), and Strain CCMP 2951 is facultatively phototrophic (requiring prey but able to grow in darkness) (Wilken et al., 2020). Xenic cultures were maintained in K medium (Keller et al., 1987) made by adding pre-mixed nutrients (NCMA) to 0.2 μm filtered coastal seawater. Because *Ochromonas* is bacterivorous, co-occurring bacteria in the xenic cultures provided a food supply, and no additional food supplementation was given. Stock cultures were kept at the ancestral

temperature of 24°C, with a 12:12 light: dark cycle and acclimated to the two experimental light levels, 100 and 50 µmol quanta m^{-2} s^{-1}, for at least 5 weeks prior to the start of the experiment.

2.2 | Evolution experiment

We conducted a long-term evolution experiment testing mixotroph responses to both 6°C lower (18°C) and higher (30°C) temperatures. This temperature range is relatively large compared to expected surface ocean temperature increases, but was chosen to maximize evolutionary responses, and is similar to temperature ranges used in other phytoplankton evolution experiments (e.g. O'Donnell et al., 2018; Padfield et al., 2016). In March 2018, we initiated six evolutionary replicates for each temperature treatment with a subpopulation of 10,000 cells from a stock culture maintained at 24°C (hereafter, "control") at each light level (Figure 1a). This initial population size was chosen over using a clonal isolate to avoid genetic bottlenecks, to increase the probability of favorable mutations, and to support the long-term stability of the cultures (Elena & Lenski, 2003; Malerba & Marshall, 2020; Wahl et al., 2002). We monitored cell density weekly by counting a live sub-sample of each lineage using a Guava easyCyte flow cytometer (Luminex Corporation), distinguishing *Ochromonas* cells using forward scatter (a proxy for cell size) and red fluorescence (a measure of photosynthetic pigmentation). Evolving cultures were transferred in a 1:15 ml dilution of fresh media in 25 ml culture flasks (Genesee Scientific; Part No. 25-212) every subsequent 2–4 weeks (depending on population density) to maintain exponential growth and maximize adaptive potential (Elena & Lenski, 2003).

2.3 | Reciprocal transplant assays

To differentiate between evolution and plasticity, we periodically transplanted evolving lineages to all treatment temperatures and quantified metabolic traits relevant to the carbon cycle (Figure 1b,c). Aliquots of evolving cultures were transferred to new temperatures for a 5-day acclimation to overcome transfer shock before experimental measurements began. We measured growth rate every 3 months to test overall fitness; photosynthetic, grazing, and respiration rates every 6 months to quantify carbon budgets; and cellular carbon and nitrogen content (yearly after Year 1 of the experiment) to determine cell size and stoichiometry. All physiological measurements were made on cells in exponential growth phase and between 5 and 10 days of temperature acclimation. We based this time window choice on preliminary data demonstrating that acclimated lineages did not display significant changes in growth rate, chlorophyll content, or photosynthetic efficiency between days 7 and 28 of acclimation to a new temperature (Figure S1). All analyses were performed using the software package R (R Core Team, 2020). Data and code are available at: https://doi.org/10.5281/zenodo.7059246.

2.4 | Growth rate and generation time

Growth assays were conducted in 24-well plates (VWR; Part No. 10062-896). On Day 6 of temperature acclimation, *Ochromonas* lineages were inoculated into 2.5 ml of media at an initial density of 20,000 cells ml^{-1} and counted daily for 4 days using a flow cytometer. Growth rates were calculated by fitting a linear model to the natural log of population size (R function *lm*). Average growth rate over

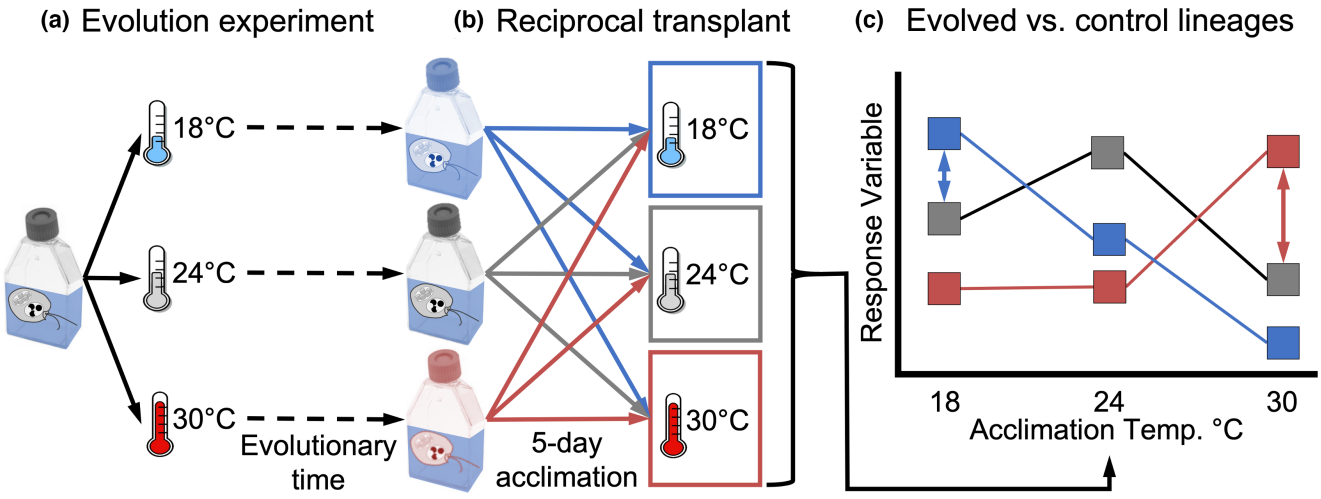

FIGURE 1 Conceptual diagram of experimental design. (a) Genetically similar ancestral cultures were split and exposed to three treatment temperatures (18, 24 [control], and 30°C), with six replicates at each temperature, for evolutionary time scales. (b) Reciprocal transplant assays were performed at regular time points, wherein aliquots of each strain were transplanted to each treatment temperature for an acclimation period of 5 days prior to trait tests to differentiate between adaptation and plasticity. (c) Hypothetical data points demonstrate the thermal reaction norms for each treatment lineage that result from reciprocal transplant assays. In particular, we can compare the cold-evolved (blue squares) and hot-evolved (red squares) to the control lineages (gray squares). Differences between these (blue and red double-sided arrows) shows evolutionary response, while no differences in thermal reaction norms (not pictured) would indicate plasticity.

the course of the experiment was estimated at 0.198 day^{-1} for all lineages which were transferred in a 1:15 dilution every 2 weeks, with the exception of the obligate phototroph at 18°C which was transferred every 4 weeks and had a growth rate 0.099 day^{-1}. These average growth rates were used to calculate generation time.

2.5 | Cellular C content

Cellular carbon (C) and nitrogen (N) content were measured using an elemental analyzer (Model CEC 440HA; Exeter Analytical). Known volumes and densities of *Ochromonas* cultures were filtered onto pre-combusted GF/F filters (Whatman Part No. 1825-025; Whatman Cytiva), acidified to remove inorganic carbonates, and dried before combustion. To control for the biomass of coexisting bacteria, bacteria-only cultures (made by inoculating media with bacteria isolated from stock *Ochromonas* cultures) at each temperature were filtered, acidified, dried and combusted. Bacteria were enumerated by plating on Difco™ Marine Broth 2216 (Becton, Dickinson and Company) agar (VWR; Part No. J637) plates. Colony forming units were counted after 7 days of incubation at 24°C, and average bacterial C content was calculated. In *Ochromonas* cultures, bacteria were similarly enumerated, and bacterial contribution of C was subtracted from the mixed-culture measurements prior to calculating *Ochromonas* cellular C content.

2.6 | Photosynthesis and respiration

Photosynthesis and respiration rates were measured using oxygen sensor spots (PyroScience) and FireStingO2 optical oxygen meters (Pyroscience; Jallet et al., 2016). *Ochromonas* were sealed into airtight glass vials with sensor spots and magnetic stir bars to keep cultures well-mixed. We monitored oxygen levels within vials continuously for 3 h in light and 2 h in darkness. To subtract respiratory contributions from coexisting bacteria, we measured respiration rates of bacteria-only cultures (see methods in Section 2.5) at all treatment temperatures. Temperature-specific bacterial respiration rates were removed from mixed cultures before calculating *Ochromonas* rates. Net photosynthesis and dark respiration rates were calculated by fitting a linear model to change in oxygen (O_2) measurements (R function *lm*) in light and darkness, respectively. Gross photosynthetic rates were computed as the sum of net photosynthesis and dark respiration, assuming that respiration rates did not change with light. We used the equation from Barton et al. (2020) to convert metabolic rates (*b*) from units of O_2 to μgC (Equation 1).

$$b\left(\mu g\,C\,\mu g\,C^{-1}\,h^{-1}\right)=\frac{b\left(\mu molO_2\,cell^{-1}\,h^{-1}\right)\times 32\times M\times\left(\frac{12}{44}\right)}{\mu g\,C\,cell^{-1}} \quad (1)$$

Equation (1) uses the molecular weights of O_2, C, and carbon dioxide (CO_2), and the species-specific assimilation quotient (*M*) from Falkowski et al. (1985). *M* describes the conversion between C and O_2 through consumption or fixation within a cell using its C:N ratio. We used estimated values for this quotient from published literature on phytoplankton Falkowski et al. (1985). This neglects possible differences between mixotrophs and phytoplankton but, so long as the quotient itself did not evolve in response to temperature, acts as a scalar that should not qualitatively affect the comparisons between *Ochromonas* strains made in this study.

2.7 | Grazing

We measured *Ochromonas* grazing rates by offering mixotrophs heat-killed fluorescently labeled bacteria (FLB; *Escherichia coli*—K-12 strain—Bioparticles®, Alexa Fluor®488 conjugate; Molecular Probes) as prey. To construct grazing functional response curves, we inoculated FLB at a range of concentrations between 0 and 4 million cells ml^{-1} into *Ochromonas* cultures, as well as into sterile media as controls. After 1 h of grazing, final concentrations of *Ochromonas* and FLB were enumerated using forward scatter, red-fluorescence, and yellow-fluorescence measurements on a flow cytometer. Grazing rates were calculated using methods of Jeong and Latz (1994) for each FLB concentration. We fit both Holling Type I (linear) and Type II (saturating) functional response curves to the data and used Akaike Information Criterion values to determine which response fit best. We then compared attack rates from the functional responses as a measure of grazing. We also estimated grazing rates by scaling to average prey densities, which were determined as average bacteria per treatment, enumerated as described in cellular C content methods.

2.8 | Photosynthetic traits

We measured electron transport rate (ETR) and photosynthetic efficiency (F_v/F_m) using a mini-Fluorescence Induction and Relaxation (miniFIRe) system (custom built by M. Gorbunov, Rutgers University, New Brunswick, NJ, USA). We quantified photosynthetic rate as a function of irradiance according to Gorbunov et al. (1999). Photosynthetic efficiency was measured as the ratio of variable to maximum fluorescence. ETR was measured at light intervals between 0 and 1000 μmol quanta m^{-2} s^{-1} to generate photosynthesis-irradiance curves, which were fit with the photosynthesis-irradiance equation of Jassby and Platt (1976) (Equation 2) using non-linear least squares regression (R function *nls*).

$$ETR=P_{max}\times\tanh\left(\frac{\alpha\times I}{P_{max}}\right) \quad (2)$$

In Equation (2), ETR is calculated using maximum ETR (P_{max}), the initial slope of ETR to light (α), and the incident irradiance (*I*). We extracted chlorophyll-*a* (chl-*a*) by incubating a known number of cells captured on a GF/F filter (Whatman Part No. 1825-025; Whatman Cytiva) overnight in 90% acetone at 4°C, then quantified it using a

Trilogy fluorometer with a 460 nm LED (Turner Designs). We used a linear model to calibrate between flow cytometry red fluorescence to extracted chl-*a* content (Figure S2). To compute per-carbon photosynthetic rates, we used the output of Equation (2) to interpolate the ETR (in electrons per molecule of chl-*a* per second) at the growth irradiance (100 µmol quanta m^{-2} s^{-1}). We then used the molecular mass of chl-*a*, the cellular chl-*a* content, and the cellular C content to convert to units of electrons per pg C per day.

2.9 | Carbon use efficiency

Carbon use efficiency was calculated to quantify how much carbon was allocated to growth. This was calculated as growth divided by the sum of growth and respiration.

2.10 | Thermal reaction norms

To obtain a more complete picture of the thermal sensitivity of metabolic traits in evolved lineages, we measured thermal reaction norms (TRNs) of photosynthesis and bacterivory. We performed photosynthesis-irradiance curves or grazing assays as described above at a range of temperatures between 3 and 44°C. These thermal assays represent short-term responses of cells to temperature where samples were incubated at the assay temperature only for the duration of the assay (15 min of dark acclimation for photosynthesis-irradiance curves; 60 min of incubation with FLB for grazing assays). For photosynthesis-irradiance curves, to rapidly bring cells to their incubation temperature, we diluted 1 ml of *Ochromonas* culture with 4 ml of sterile, filtered seawater at the assay temperature. We only collected TRN data from the obligate phototroph (Strain 1391) evolved at high light because this strain showed the strongest adaptive response to temperature. TRNs for ETR were fit using a reparameterized version of the Norberg-Eppley equation (Equation 3) from the R package "growthTools" (Kremer, 2021).

$$\mu = e^{(a+bT)}\left[1-\left(\frac{-2-2bT_{opt}+2bT+\left[4+bw^2\right]^{\frac{1}{2}}}{bw}\right)^2\right] \quad (3)$$

In Equation (3), μ is the metabolic trait, T is temperature, T_{opt} is the optimum temperature, a affects the y-intercept, b affects thermal scaling, and w describes the thermal niche width. For photosynthetic efficiency and grazing, we added smoothed conditional means (R function *ggplot2::geom_smooth*).

2.11 | Transcriptome sequencing

Finally, we measured gene expression in the obligate phototroph (Strain 1391) evolved at high light to better understand cellular mechanisms underlying observed adaptive responses. To contrast evolved and acclimatory responses, we collected transcriptomes from lineages evolving at all temperatures, and from control lineages evolving at 24°C but acclimated to 18 or 30°C. In week 141 of the experiment, we inoculated exponentially growing *Ochromonas* cells into 130 ml volumes of culture media in 250 ml tissue culture flasks (VWR; Part No. 10062-860). We incubated these cultures for 48 h at their evolutionary temperatures (to allow cells to overcome transfer shock), before transplanting acclimation treatments to their new temperatures. Evolving treatments remained at their initial temperatures. After 7 days (the mean acclimation time of our reciprocal transplant studies; see above), we filtered the cultures onto 0.8 µm pore size polycarbonate filters (Millipore ATTP04700; Millipore Sigma), immediately flash-froze samples in liquid nitrogen, and then stored them at −80°C until RNA extraction (within 1 week). We collected one transcriptome from each evolving or acclimated lineage (=5 treatments × 6 replicates for a total of 30 samples), except for lineages evolving at 18°C for which we collected technical triplicates (i.e. inoculated three replicate 130 ml volumes of media, and collected three replicate transcriptomes) to contrast the range of gene expression in technical replicates with that contained amongst biological replicates.

We extracted samples using an RNeasy Plant Mini Kit (Qiagen). Cells were physically disrupted by adding 2.8 mm ceramic beads (Qiagen) and 400 µl Buffer RLT with 10 µl/ml β-mercaptoethanol (Qiagen), then vortexed for 30 s. Following cell lysis, RNA extraction proceeded according to the manufacturer's instructions. Samples were sequenced and cDNA preparation was performed at the UC Davis DNA Technologies Core (Davis, CA, USA) on two lanes of an Illumina NovaSeq (PolyA pulldown NovaSeq S4 PE150). We assembled uncorrected reads de novo with RNA SPAdes (v3.13.0; default parameters, k = 49, 73) (Bankevich et al., 2012) and used TransDecoder (v5.5.0) to translate assemblies into protein sequences. We compared our predicted proteins with the NCBI RefSeq database using Diamond v2.02 (-p 32 -b 8 -c 1) (Buchfink et al., 2015); Sequences that were identified as bacterial (>90% sequence identity and >80% query coverage) were considered contaminants and removed from further analysis. We then assessed assembly completeness using Busco v 5.0.0 (Simão et al., 2015) and used KEGG GhostKoala (Kanehisa et al., 2016) to perform preliminary annotations. Read mappings to nucleotide transcripts were quantified with Salmon 0.12.0 (-l A --validateMappings --gcBias) (Patro et al., 2017), and differential expression was analyzed with the R package DEseq2 v1.28.1 (Love et al., 2014). Differential expression was calculated with Approximate Posterior Estimation for GLM (*apeglm*) (Zhu et al., 2019).

To quantify the effects of evolutionary history on gene expression, we first confirmed that single replicate transcriptomes were sufficient to capture variation in gene expression within treatment group. We did this by contrasting differential expression within technical replicates and across biological replicates for lineages evolved at 18°C. Next, we identified genes with evidence of differential expression (>2× change in expression; adjusted p-value <.1) across

any treatment group and asked whether differentially expressed genes tended to be up- or down-regulated in response to temperature. To study genes linked to thermal evolution, we selected genes with differential expression between *either* lineages evolved at 18°C and those acclimated to 18°C *or* lineages evolved at 30°C and those acclimated to 30°C. We then contrasted expression in this subset of genes in thermally evolved or acclimated lineages with control lineages.

3 | RESULTS

3.1 | Obligate phototroph growth rates evolved in response to temperature

We found evidence for thermal adaptation in the obligate phototroph, *Ochromonas* Strain 1391, when it was evolved in high light (100 µmol quanta m^{-2} s^{-1}) at both cold and hot temperatures (Figure 2a). Within 50 generations, evolving lineages grew faster than the acclimated controls (lineages evolving at ancestral temperatures and assayed at the evolutionary temperature, Figure S3). Evidence for adaptation in the obligate phototroph was weaker at the lower light level (50 µmol quanta m^{-2} s^{-1}), which showed significant relative increases in growth rate at cold temperatures after about 50 generations, but mixed evidence for adaptation at hot temperatures (4 out of 11 reciprocal transplant experiments showed increases in growth, Student's *t*-test, Figure 2b). Growth rates of the facultative phototroph, *Ochromonas* Strain 2951, were much more variable, and did not show consistent evidence of evolution in any direction (Figure 2c,d).

3.2 | Evolution affects mixotroph traits

Although only the obligate phototroph showed strong evidence for adaptation over time (in the form of increases in growth rates relative to the acclimated controls), all mixotroph strains displayed evolutionary responses to temperature in carbon cycle-relevant traits. Generally, evolutionary thermal responses were less variable than phenotypically plastic ones (Figure 3). By year three of the

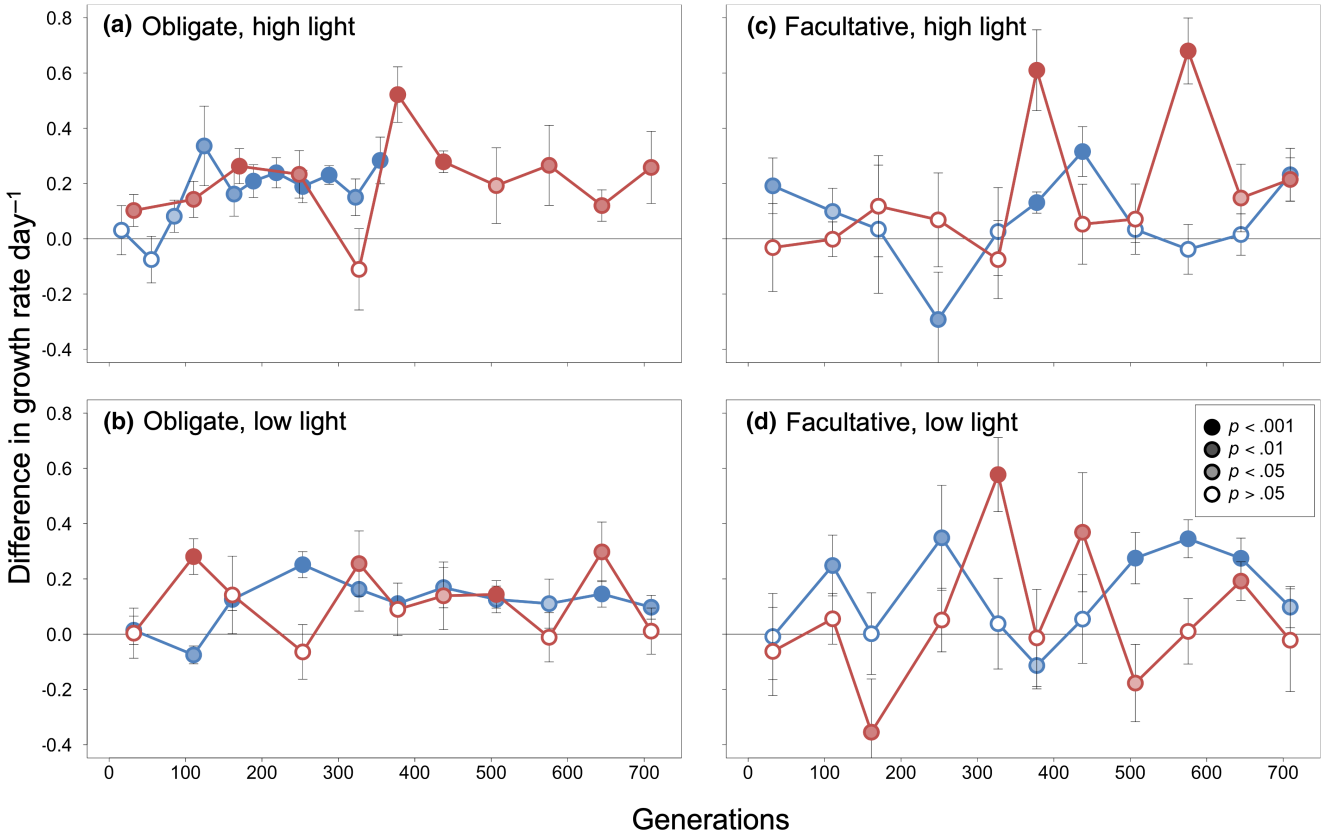

FIGURE 2 Thermal adaptation in obligate phototrophs. To test for evolutionary responses, we computed the difference in growth rates between experimental and acclimated control lineages at hot (red) and cold (blue) temperatures. Positive values are evidence of adaptive evolution (experimental lineages growing faster than acclimated control lineages assayed at the same temperature). The *x*-axes are scaled by growth rate to show time in number of generations the evolving strains experienced at their evolutionary temperatures. Data are shown for both mixotroph strains—the obligate phototroph Strain 1391 (left column) and the facultative phototroph Strain 2951 (right column)—and both light levels—high light (100 µmol quanta m^{-2} s^{-1} top row), and low light (50 µmol quanta m^{-2} s^{-1}, bottom row) for each reciprocal transplant experiment. Point coloration indicates significance ranging from $p < .001$ (darkest points; one sample Student's *t*-test) to $p > .05$ (white).

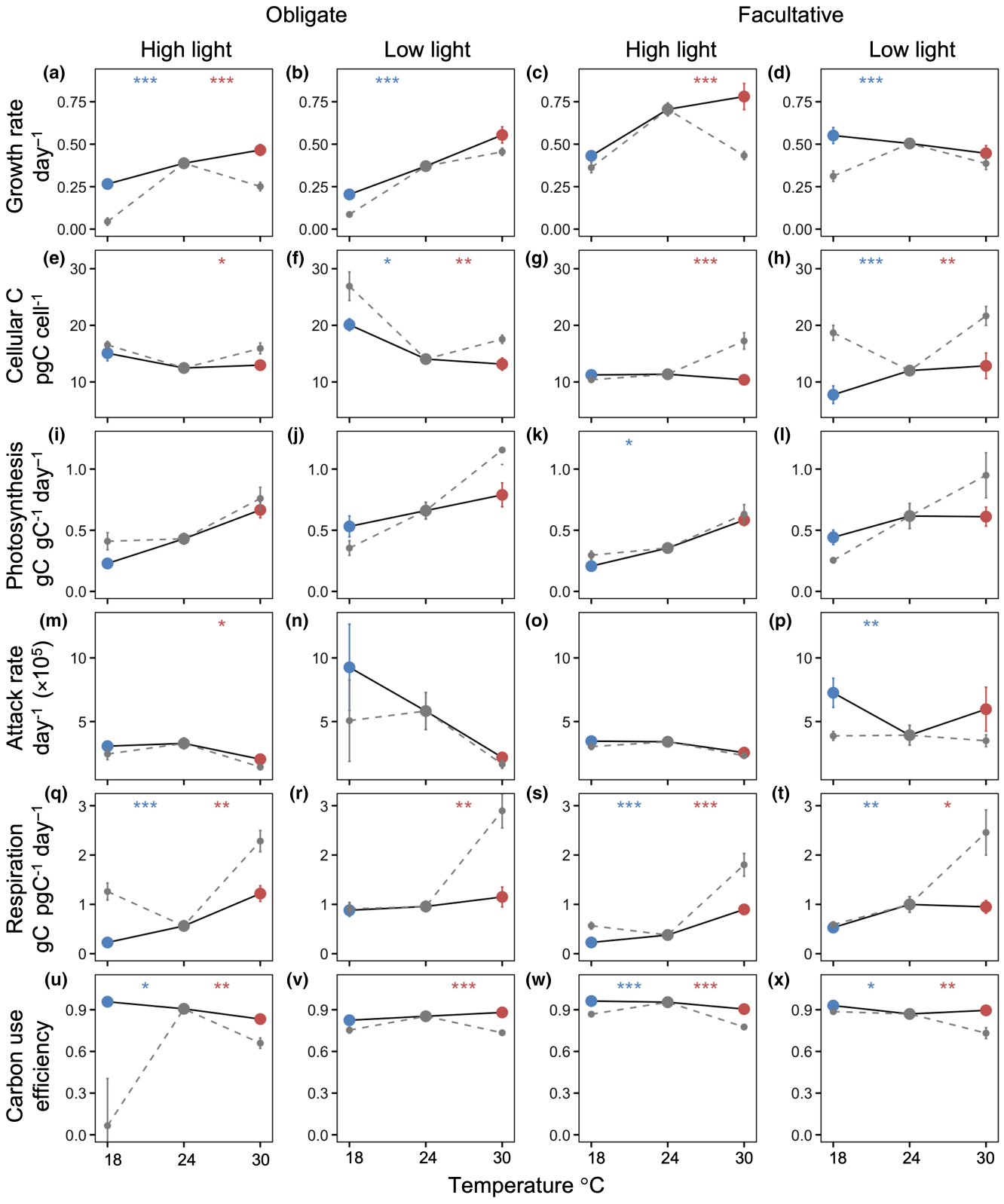

FIGURE 3 Thermal responses of carbon cycle-relevant traits in mixotrophs. We measured the plastic response of control lineages acclimated to all temperatures (gray points, dotted lines) and the evolved response of experimental lineages at their treatment temperatures (cold-evolved in blue, hot-evolved in red, solid black line). Data for the obligate (Strain 1391, first and second column) and the facultative phototroph (Strain 2951, third and fourth column) are shown for both light levels (high light in first and third column, low light in second and fourth column). Points represent means for all six replicates across the final year of the project (2–3 time points) of the experiment, with error bars showing ±1 standard error. We measured growth rate (a–d), cellular carbon content (e–h), photosynthesis (i–l), attack rate (m–p), respiration (q–t), and carbon use efficiency (u–x). Significant differences between the evolved and acclimated response at treatment temperatures are shown at the top of each panel in blue for 18°C and red for 30°C (two-sample Student's *t*-test; ***$p < .001$, **$p < .01$, and *$p < .05$).

experiment, most lineages showed some evidence of adaptation through increased growth rate compared to acclimated controls (Figure 3, top row), though note that this represents three time points that are part of a more equivocal trend in the facultative phototroph. As a result, evolution produced a general trend of increasing growth rates with ambient temperature (true after evolution in all lineages except the facultative phototroph at low light, Figure 3, top row). For obligate phototrophs, cellular C content generally decreased with temperature in evolved lineages (Figure 3, second row), though this was driven by higher carbon contents at the coldest temperature. In all cases, mixotrophs evolved towards lower carbon content at the hottest temperatures relative to phenotypic plasticity in the control (Figure 3, second row, compare red and gray points). Forward scatter (a proxy for physical size) also tended to decrease with temperature, but did not vary with evolution except when the obligate phototroph was evolved at high light (Figure S4, bottom row).

Evolutionary responses in photosynthesis and grazing were more variable. The TRNs of photosynthesis were most affected by evolution at the lowest light level, becoming less steep (higher photosynthetic rates at cold temperatures; lower photosynthetic rates at hot temperatures) after 3 years of evolution (Figure 3, row 3). This may have resulted in part from a similar flattening of thermal reactions norms of chlorophyll at low light levels (Figure S4b,d), and due to changes in the use of photosynthetic machinery, especially increases in photosynthetic efficiency at low temperatures (Figure S4). The TRNs of attack rate were flatter in all treatments except the facultative phototroph at low light, though most differences between adapted and evolved lineages were not statistically significant (Figure 3, row 4). We also estimated grazing rates based on average bacterial rates counted within each treatment flask as prey abundance in these systems may affect overall heterotrophy. Though our methods of assessing grazing make the assumption that all prey are equally palatable and may underestimate the number of prey based on enumeration through plating, they are still likely to be qualitatively consistent between treatments. These grazing rates decreased slightly with temperature in evolved lineages, and TRNs were flatter in high light treatments (Figure S4, row 3).

Overall, respiration rates decreased in evolved strains compared to acclimated control strains (Figure 3, row 5), except when lineages were evolved to lower temperatures at low light. This resulted in marked increases in carbon use efficiency across evolved lineages (Figure 3, row 6).

3.3 | Mechanisms underlying adaptation in obligate phototroph at high light

For the obligate phototroph at high light (which had the strongest evidence for adaptive evolution), metabolic and transcriptomic differences indicate evolutionary changes to cellular processes that may underlie adaptation. In the hot-evolved obligate phototroph, increased growth rates at the hot temperature (Figure 4a) were driven by a 19% reduction in cell size (Figure 4b), a 43% increase in attack rate (Figure 4e), and a 46% decrease in respiratory costs (Figure 4f) relative to the acclimated control. Although chlorophyll content normalized to cell size increased in the hot-evolved lineages (Figure 4c), total carbon fixation was slightly lower (Figure 4d). In cold-evolved lineages, cell sizes and attack rates did not vary significantly from the control at cold temperatures (Figure 4b,e), but increased growth rates may have been driven by an 80% decrease in respiratory costs (Figure 4f).

In the obligate phototroph at high light, cold- and hot-evolved lineages showed changes in the TRNs for two important photosynthetic traits. Hot-evolved lineages had lower ETR per carbon at nearly all temperatures than those evolved at lower temperatures (Figure 5a), but maintained photosynthetic efficiency to higher temperatures (Figure 5b). The photosynthetic rates of cold-evolved lineages were more sensitive to changes in temperature (had steeper initial thermal response curve of ETR) and generally had lower photosynthetic efficiency (Figure 5b). The grazing thermal response curves showed some signs of shifts in thermal optima but had much higher variability between replicates within the same treatment (Figure S5).

Finally, we used our transcriptome data to understand changes in gene expression underlying our observed physiological responses. First, we confirmed that variation amongst our biological replicates exceeded any variation captured by technical replication (Figure S6). We then proceeded with a comparative analysis using only one transcriptome per lineage. We found that, although some variation in gene expression existed across biological replicates, gene expression varied strongly by treatment (Figure S7; Table S1). Of the 17,140 *Ochromonas* gene transcripts that we identified, we found that 6951 genes were differentially expressed between lineages evolved at and adapted to 30°C. Of these, 380 genes had >2-fold upregulation, and 147 had >2-fold downregulation. Of 5420 genes differentially expressed between lineages evolved at and adapted to 18°C, 105 had >2-fold upregulation, and 142 had >2-fold downregulation. Among these differentially expressed genes, we found evidence across metabolic pathways for a return to "baseline" gene expression levels over evolutionary time (Figure 6). Specifically, cultures that experienced a 7-day acclimation to new temperatures tended to exhibit down-regulation when expression levels were compared to lineages evolved and acclimated at 24°C (Figure 6). In contrast, evolved lineages had broadly similar gene expression levels across temperatures (Figure 6; Figure S6).

4 | DISCUSSION

Mixotrophs play an integral role in oceanic food webs and the biological carbon pump (Caron, 2016; Mitra et al., 2014; Ward & Follows, 2016; Worden et al., 2015) and are predicted to become more heterotrophic with rising temperatures (Allen et al., 2005; Wilken et al., 2013). However, such predictions fail to account for evolutionary responses. We found that mixotrophs, like other unicellular organisms with fast generation times (Kawecki et al., 2012),

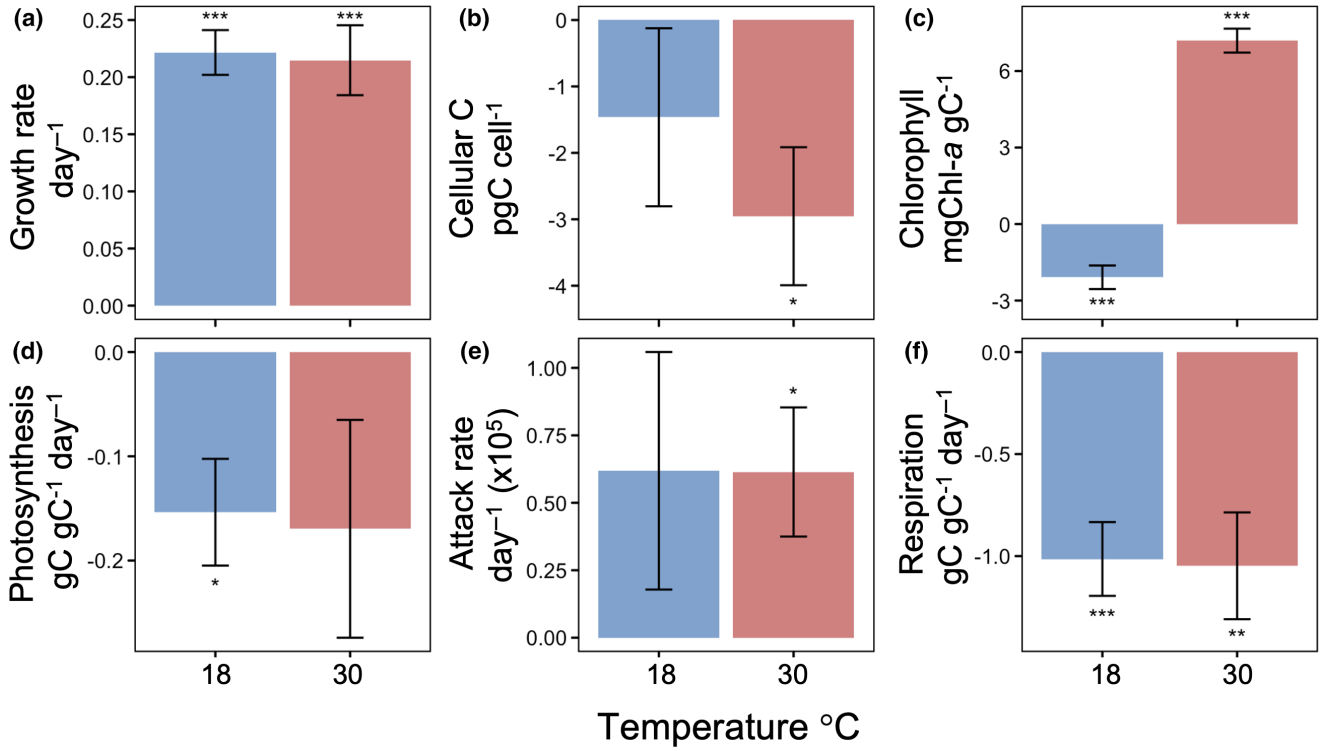

FIGURE 4 Differences between evolved and plastic responses of obligate phototroph at high light. Differences between evolved responses of the cold and warm evolved lineages and the plastic responses of the acclimated controls at the respective cold and warm temperatures (obtained from reciprocal transplant) are shown for several key traits, to examine what mechanisms drove adaptation in the obligate phototroph (Strain 1391) at high light (100 μmol quanta m^{-2} s^{-1}). The differences in cold-evolved lineages and acclimated controls are shown in blue, and the differences in hot-evolved lineages and acclimated controls is shown in red. Data are averaged for all six replicates across the last year of the experiment (2–3 time points) with error bars showing ±1 standard error. We measured growth rate (a), cellular C content (b), chlorophyll (c), photosynthesis (d), attack rate (e), and respiration (f). Significant differences are shown by each bar (one-sample Student's *t*-test; *** $p < .001$, ** $p < .01$, and * $p < .05$).

can adapt to new thermal conditions within 50 generations, but that the magnitude of adaptation varied by mixotroph identity and environmental conditions. Generally, mixotrophs evolved lower respiration rates and higher carbon use efficiencies, responses that paralleled similar evolution experiments conducted in phytoplankton (Barton et al., 2020; Padfield et al., 2016; Schaum et al., 2018). At higher temperatures, mixotrophs evolved lower rates of photosynthesis and higher rates of grazing, compounding metabolic scaling predictions that mixotrophs will become more heterotrophic as temperatures increase (Princiotta et al., 2016; Rose & Caron, 2007; Wilken et al., 2013).

Two competing processes shaped the consequences of mixotroph evolution on carbon cycling. On the one hand, evolved lineages had lower photosynthetic rates, higher attack (and grazing) rates, and smaller cell sizes compared to control lineages at hot temperatures (Figures 3 and 4; Figure S4), suggesting mixotroph evolution could compound carbon dioxide atmospheric accumulation. On the other hand, evolved lineages also exhibited reduced respiration and higher carbon use efficiencies (Figures 3 and 4), suggesting that mixotrophs could increase trophic transfer efficiency and, potentially, carbon export (Ward & Follows, 2016). However, we were unable to balance the mixotrophs' carbon budget as carbon uptake (through photosynthesis and grazing) did not consistently match the sum of respiration and growth. One possible missing flux is the loss of organic carbon through leakage or exudation (Thornton, 2014). Because we did not monitor pH evolution (except to confirm that pH did not change appreciably during exponential growth phase), alkalinity, or dissolved carbon within our cultures, we could not quantify this loss or how much carbon dioxide was absorbed through diffusion. Evidence suggests that *Ochromonas* likely do not have a carbon concentrating mechanism (CCM, Maberly et al., 2009), although transcriptomic analysis shows that some strains retain the genes coding for proteins related to a CCM (Lie et al., 2018). Additionally, our method of assessing grazing may be biased by differences in palatability of prey, as well as underestimating total bacteria populations based on the growth medium.

In general, evolved metabolic rates shifted back towards ancestral rates as they adapted, suggesting a recovery from stress-induced dysregulation to homeostasis. Stress has been shown to cause physiological and metabolic dysregulation in marine organisms (Fernández-Pinos et al., 2017; Innis et al., 2021). In our experiment, when mixotrophs were briefly acclimated to new thermal environments, they exhibited similar dysregulation of metabolism (either increases or decreases in metabolic rates relative to the 24°C control

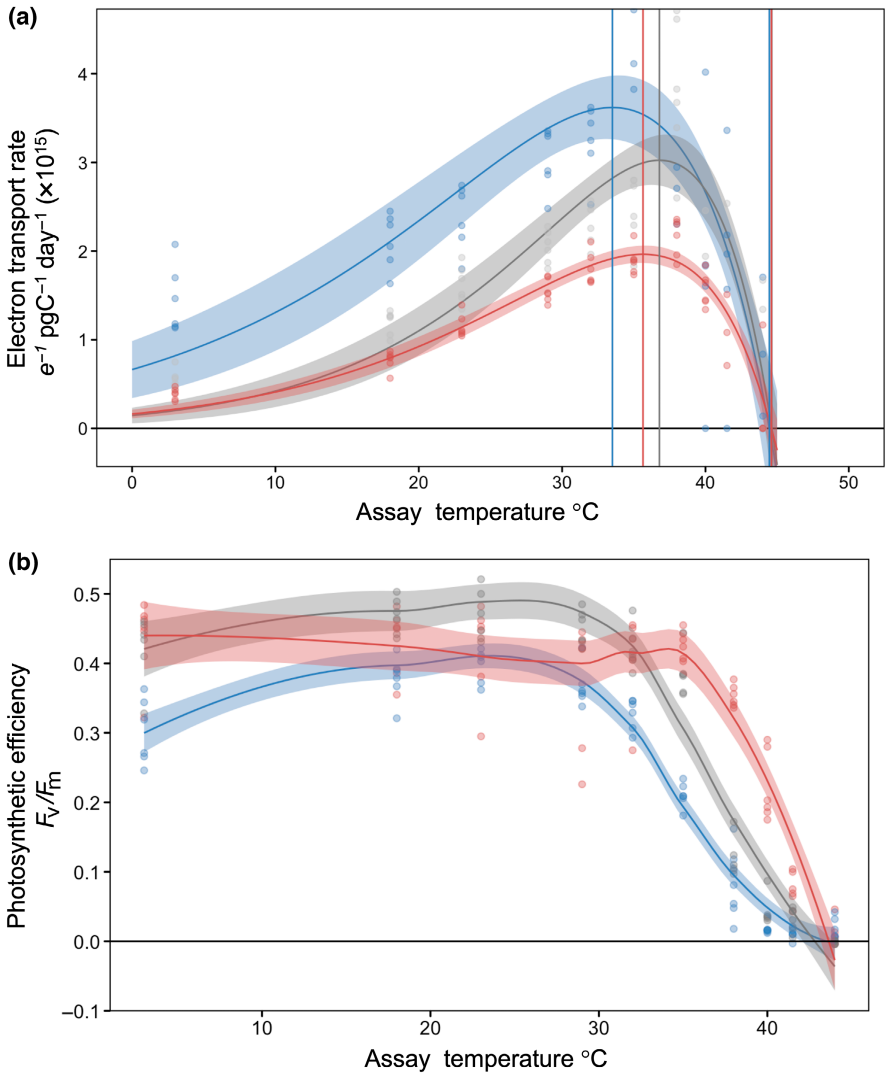

FIGURE 5 Thermal response curves of two photosynthetic traits for obligate phototroph at high light. Electron transport rate per pgC (a) and photosynthetic efficiency (b) were measured at 10 temperatures between 3 and 44°C for cold-evolved (blue), control (gray), and hot-evolved (red) lineages at the termination of the evolution experiment. For the cold-evolved lineages this represents >200 generations, and for the hot-evolved lineages, this represents >600 generations. Curves with confidence intervals represent the average of all six lineages at each temperature and individual lineages are represented by points. Three vertical lines farthest to the left represent the thermal optimum of each temperature, while the vertical lines on the right represent the thermal maxima.

lineages; Figure 3, gray lines) and gene expression (reduced expression; Figure 6a, gray histograms). Yet over evolutionary time, mixotrophs adapted to the altered temperatures, such that evolved TRNs were flatter than acclimatized ones (Figure 3, compare "flatter" gray to "steeper" black lines) and relative gene expression levels returned to the optimized expression of the control (Figure 6a, blue and red histograms). This suggests that mixotrophs experience short-term acclimations as a "shock" that induces a stress response, but over time evolution allows them to recover by returning to an adaptive steady state homeostasis. The return to homeostasis in transcription regulation parallels other microbial systems (Brauer et al., 2008; López-Maury et al., 2008), including thermal response in *Escherichia coli* (Ying et al., 2015), suggesting global transcriptome optimization is a key component of adaptive thermal evolution. Evolved recovery from stress through the reversal of plastic responses has also been found in green algae in response to elevated CO_2 (Schaum & Collins, 2014).

Although all the mixotrophic lineages we evolved exhibited some evolutionary responses (Figure 3), only the obligate phototroph (*Ochromonas* Strain 1391) showed consistent evidence for adaptation (Figure 2). The facultative phototroph's (Strain 2951) higher innate phenotypic plasticity may have resulted in a more muted evolutionary response: If the temperatures tested in our evolution experiment fell within Strain 2951's capacity for plastic responses, this strain could have experienced reduced selection pressure compared to Strain 1391 (Snell-Rood et al., 2010). These findings intersect with a larger literature exploring the relationship between phenotypic plasticity and rapid evolution: More plastic lineages may be better able to survive in changing environments, thus "buying time" to evolve new adaptations (West-Eberhard, 2003). But plasticity may also inhibit evolution when it inhibits the fixation of adaptive traits (Whitlock, 1996). Because our study used only two mixotroph strains, we urge caution in interpreting our results in this context. However, constitutive mixotrophs fall along a wide spectrum of phenotypic plasticity, so future work could use this system as a testbed for these ideas.

Mixotroph evolution may also have been constrained by selection pressures imposed by our experimental design. For example, our experiment was conducted using warm water-adapted species (from an ancestral temperature of 24°C) that may have already been near the upper limits of thermal tolerance (Thomas et al., 2012). Thus, while the cold-evolved lineages of the obligate phototroph shifted

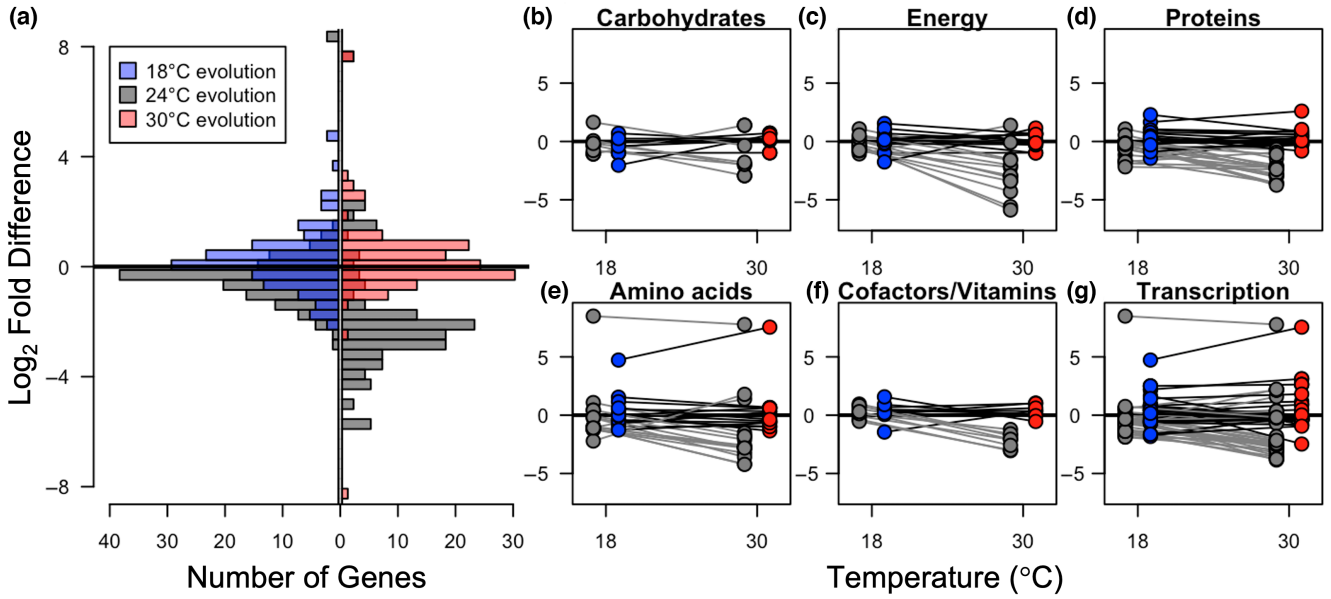

FIGURE 6 Evolution returns gene expression to homeostasis. (a) Differences in expression of annotated genes between evolved and acclimated lineages at 18°C (left) and 30°C (right) compared to the control (24°C) lineages acclimated at 24°C. Across genes that were significantly differentially expressed, we observed a tendency towards downregulation in acclimated lineages (gray; left side are acclimated to 18°C, right side are acclimated to 30°C), while evolved lineages tended to have gene expression levels similar to one another regardless of temperature (blue and red). (b–g) This pattern was evident in many metabolic pathways (lines connect data from individual gene candidates), especially those associated with energy metabolism and biosynthesis. Colored points represent evolved lineages (blue = 18°C; red = 30°C), and gray points represent control lineages acclimated to hot and cold temperatures.

their photosynthetic thermal optima to slightly lower temperatures, the thermal optima for hot-evolved lineages did not change, and the thermal maxima were similar for all evolved lineages (Figure 5). This supports the idea that thermal maxima that are physiologically constrained by metabolic limits are strongly phylogenetically conserved (Araújo et al., 2013). We also conducted our experiment in replete nutrient conditions and under stable temperature and light environments. In reality, nutrient limitation—which is likely experienced by mixotrophs in oligotrophic gyre habitats—can inhibit evolutionary adaptation (Aranguren-Gassis et al., 2019; Marañón et al., 2018; Thomas et al., 2017), as can the combination of multiple stressors (Brennan & Collins, 2015). Additionally, our evolving lineages were xenic. Thus, bacterial prey in our experiment coevolved with the *Ochromonas* lineages. While this "community evolution" is a realistic scenario in marine ecosystems, this means that evolutionary changes in bacterial prey could have created complex feedbacks in prey availability and palatability, and may have affected our grazing rate estimates.

Finally, we note that our interpretation of our results as evidence for mixotroph evolution is shaped by our choice of reference point. In this experiment, we used lineages evolved at 24°C, and then briefly acclimated to both colder and hotter temperatures, as our "control" for phenotypic plasticity. While our preliminary tests suggested that mixotroph phenotypes were consistent over the first few weeks of acclimation to new temperatures (Figure S1), without evidence of genotypic change, it remains challenging to differentiate between transient acclimation dynamics, phenotypic plasticity, and a true evolutionary response. Other studies have used longer acclimation windows of 2 weeks or at least 10 generations to establish full acclimation to new conditions (Staehr & Birkeland, 2006; Trimborn et al., 2014). In contrast, in our cold-temperature acclimations, markedly reduced growth rates of acclimating strains mean that a 5-day acclimation window could represent as few as two generations. Thus, an alternative interpretation of our findings could be that our "control" data actually represent a short-term stress-response, though we note that long-term acclimation data suggest this response persists for at least 4 weeks (>8 generations) in our control lineages (Figure S1). Our choice of reference point also impacted our interpretation of the speed of mixotroph adaptive evolution. Other studies have shown that phytoplankton can mount an adaptive response in <50 generations (Malerba et al., 2018), though the speed and magnitude of adaptation are impacted by the availability of nutrients (Aranguren-Gassis et al., 2019) and co-occurring stressors (Brennan et al., 2017). The speed and consistency (i.e. that the six replicate evolving lineages were phenotypically and transcriptionally similar to one another) of adaptation in our study may have resulted from our choice to start with a mixed (rather than clonal) population: Perhaps a single genotype from the original mixture swept to numerical dominance during the course of the experiment. Future studies should contrast our findings with other experimental designs, including higher temporal resolution of sampling, and initialization with clonal and/or axenic mixotroph populations.

In sum, our findings highlight the complex interaction between mixotroph identity and environmental selection pressures in

constraining marine plankton adaptation. While some general trends (increased carbon use efficiency; flattening of TRNs; return to homeostatic gene expression) emerged, evolutionary responses were highly context dependent. These results suggest that incorporating evolutionary responses of marine microbes into climate predictions will be challenging. Additional studies may allow us to better link organismal metabolic plasticity to evolutionary responses and develop a more robust framework to predict the structure and function of upper ocean communities.

AUTHOR CONTRIBUTIONS

Michelle Lepori-Bui and Holly V. Moeller designed the study, conducted experiments, analyzed data, and wrote the manuscript. Christopher Paight conducted transcriptomic lab work and analyses. Conner M. Mertz and Ean Eberhard developed protocols and conducted experiments. All authors contributed to manuscript revisions.

ACKNOWLEDGMENTS

We thank Sandeep Venkataram for discussions that shaped study design. We gratefully acknowledge manuscript feedback from Suzana Leles, Erika Eliason, Debora Iglesias-Rodriguez, and the members of the Moeller Lab at UC Santa Barbara. We thank Ryan Marczak, Gina Barbaglia, and Veronica Hsu for laboratory assistance, and the members of the Eliason Lab at UC Santa Barbara for lending us equipment and helping with early methods development. This manuscript benefited greatly from the comments of several anonymous reviewers. This work was funded by the National Science Foundation under grant NSF OCE-1851194 (to HVM).

CONFLICT OF INTEREST

The authors declare no conflict of interest.

DATA AVAILABILITY STATEMENT

Sequence reads have been uploaded to NCBI (sample numbers: SAMN25046786–SAMN25046826) and the SRA will be available when the manuscript is accepted. Scripts and data are available at: https://doi.org/10.5281/zenodo.7059246.

ORCID

Michelle Lepori-Bui https://orcid.org/0000-0002-1239-8824
Christopher Paight https://orcid.org/0000-0002-0286-8837
Ean Eberhard https://orcid.org/0000-0002-7264-8143
Conner M. Mertz https://orcid.org/0000-0001-8710-212X
Holly V. Moeller https://orcid.org/0000-0002-9335-0039

REFERENCES

Allen, A. P., Gillooly, J. F., & Brown, J. H. (2005). Linking the global carbon cycle to individual metabolism. *Functional Ecology*, *19*, 202–213.

Aranguren-Gassis, M., Kremer, C. T., Klausmeier, C. A., & Litchman, E. (2019). Nitrogen limitation inhibits marine diatom adaptation to high temperatures. *Ecology Letters*, *22*, 1860–1869.

Araújo, M. B., Ferri-Yáñez, F., Bozinovic, F., Marquet, P. A., Valladares, F., & Chown, S. L. (2013). Heat freezes niche evolution. *Ecology Letters*, *16*, 1206–1219.

Bankevich, A., Nurk, S., Antipov, D., Gurevich, A. A., Dvorkin, M., Kulikov, A. S., Lesin, V. M., Nikolenko, S. I., Pham, S., Prjibelski, A. D., Pyshkin, A. V., Sirotkin, A. V., Vyahhi, N., Tesler, G., Alekseyev, M. A., & Pevzner, P. A. (2012). SPAdes: A new genome assembly algorithm and its applications to single-cell sequencing. *Journal of Computational Biology*, *19*, 455–477.

Barton, S., Jenkins, J., Buckling, A., Schaum, C.-E., Smirnoff, N., Raven, J. A., & Yvon-Durocher, G. (2020). Evolutionary temperature compensation of carbon fixation in marine phytoplankton. *Ecology Letters*, *23*, 722–733.

Brauer, M. J., Huttenhower, C., Airoldi, E. M., Rosenstein, R., Matese, J. C., Gresham, D., Boer, V. M., Troyanskaya, O. G., & Botstein, D. (2008). Coordination of growth rate, cell cycle, stress response, and metabolic activity in yeast. *Molecular Biology of the Cell*, *19*, 352–367.

Brennan, G. L., Colegrave, N., & Collins, S. (2017). Evolutionary consequences of multidriver environmental change in an aquatic primary producer. *Proceedings of the National Academy of Sciences*, *114*, 9930–9935.

Brennan, G., & Collins, S. (2015). Growth responses of a green alga to multiple environmental drivers. *Nature Climate Change*, *5*, 892–897.

Brown, J. H., Gillooly, J., Allen, A. P., Savage, V., & West, G. (2004). Toward a metabolic theory of ecology. *Ecology*, *85*, 1771–1789.

Buchfink, B., Xie, C., & Huson, D. H. (2015). Fast and sensitive protein alignment using DIAMOND. *Nature Methods*, *12*, 59–60.

Caron, D. A. (2016). Mixotrophy stirs up our understanding of marine food webs. *Proceedings of the National Academy of Sciences of the United States of America*, *113*, 2806–2808.

Collins, S., Rost, B., & Rynearson, T. A. (2014). Evolutionary potential of marine phytoplankton under ocean acidification. *Evolutionary Applications*, *7*, 140–155.

Elena, S. F., & Lenski, R. E. (2003). Evolution experiments with microorganisms: The dynamics and genetic bases of adaptation. *Nature Reviews. Genetics*, *4*, 457–469.

Falkowski, P. G., Dubinsky, Z., & Wyman, K. (1985). Growth-irradiance relationships in phytoplankton1. *Limnology and Oceanography*, *30*, 311–321.

Fernández-Pinos, M.-C., Vila-Costa, M., Arrieta, J. M., Morales, L., González-Gaya, B., Piña, B., & Dachs, J. (2017). Dysregulation of photosynthetic genes in oceanic *Prochlorococcus* populations exposed to organic pollutants. *Scientific Reports*, *7*, 8029.

Gillooly, J. F., Brown, J. H., West, G. B., Savage, V. M., & Charnov, E. L. (2001). Effects of size and temperature on metabolic rate. *Science*, *293*, 2248–2251.

Gorbunov, M. Y., Kolber, Z. S., & Falkowski, P. G. (1999). Measuring photosynthetic parameters in individual algal cells by fast repetition rate fluorometry. *Photosynthesis Research*, *62*, 141–153.

Hartmann, M., Grob, C., Tarran, G. A., Martin, A. P., Burkill, P. H., Scanlan, D. J., & Zubkov, M. V. (2012). Mixotrophic basis of Atlantic oligotrophic ecosystems. *Proceedings of the National Academy of Sciences*, *109*, 5756–5760.

Innis, T., Allen-Waller, L., Brown, K. T., Sparagon, W., Carlson, C., Kruse, E., Huffmyer, A. S., Nelson, C. E., Putnam, H. M., & Barott, K. L. (2021). Marine heatwaves depress metabolic activity and impair cellular acid–base homeostasis in reef-building corals regardless of bleaching susceptibility. *Global Change Biology*, *27*, 2728–2743.

Jallet, D., Caballero, M. A., Gallina, A. A., Youngblood, M., & Peers, G. (2016). Photosynthetic physiology and biomass partitioning in the model diatom *Phaeodactylum tricornutum* grown in a sinusoidal light regime. *Algal Research*, *18*, 51–60. https://doi.org/10.1016/j.algal.2016.05.014

Jassby, A. D., & Platt, T. (1976). Mathematical formulation of the relationship between photosynthesis and light for phytoplankton. *Limnology and Oceanography*, *21*, 540–547.

Jeong, H., & Latz, M. (1994). Growth and grazing rates of the heterotrophic dinoflagellates *Protoperidinium* spp. on red tide dinoflagellates. *Marine Ecology Progress Series*, *106*, 173–185.

Kanehisa, M., Sato, Y., & Morishima, K. (2016). BlastKOALA and GhostKOALA: KEGG tools for functional characterization of genome and metagenome sequences. *Journal of Molecular Biology*, *428*, 726–731.

Kawecki, T. J., Lenski, R. E., Ebert, D., Hollis, B., Olivieri, I., & Whitlock, M. C. (2012). Experimental evolution. *Trends in Ecology & Evolution*, *27*, 547–560.

Keller, M. D., Selvin, R. C., Claus, W., & Guillard, R. R. L. (1987). Media for the culture of oceanic ultraphytoplankton. *Journal of Phycology*, *23*, 633–638.

Kremer, C. T. (2021). *growthTools: Tools for analyzing time series of microbial abundances to estimate growth rates*. R package version 0.1.1.9000. https://github.com/ctkremer/growthTools

Lie, A. A. Y., Liu, Z., Terrado, R., Tatters, A. O., Heidelberg, K. B., & Caron, D. A. (2018). A tale of two mixotrophic chrysophytes: Insights into the metabolisms of two *Ochromonas* species (Chrysophyceae) through a comparison of gene expression. *PLoS One*, *13*, e0192439.

Listmann, L., LeRoch, M., Schlüter, L., Thomas, M. K., & Reusch, T. B. H. (2016). Swift thermal reaction norm evolution in a key marine phytoplankton species. *Evolutionary Applications*, *9*, 1156–1164.

Love, M. I., Huber, W., & Anders, S. (2014). Moderated estimation of fold change and dispersion for RNA-seq data with DESeq2. *Genome Biology*, *15*, 550.

López-Maury, L., Marguerat, S., & Bähler, J. (2008). Tuning gene expression to changing environments: From rapid responses to evolutionary adaptation. *Nature Reviews. Genetics*, *9*, 583–593.

Maberly, S. C., Ball, L. A., Raven, J. A., & Sültemeyer, D. (2009). Inorganic carbon acquisition by Chrysophytes. *Journal of Phycology*, *45*, 1052–1061.

Malerba, M. E., & Marshall, D. J. (2020). Testing the drivers of the temperature–size covariance using artificial selection. *Evolution*, *74*, 169–178.

Malerba, M. E., Palacios, M. M., Palacios Delgado, Y. M., Beardall, J., & Marshall, D. J. (2018). Cell size, photosynthesis and the package effect: An artificial selection approach. *New Phytologist*, *219*, 449–461.

Marañón, E., Lorenzo, M. P., Cermeño, P., & Mouriño-Carballido, B. (2018). Nutrient limitation suppresses the temperature dependence of phytoplankton metabolic rates. *The ISME Journal*, *12*, 1836–1845.

Mitra, A., Flynn, K. J., Burkholder, J. M., Berge, T., Calbet, A., Raven, J. A., Granéli, E., Glibert, P. M., Hansen, P. J., Stoecker, D. K., Thingstad, F., Tillmann, U., Våge, S., Wilken, S., & Zubkov, M. V. (2014). The role of mixotrophic protists in the biological carbon pump. *Biogeosciences*, *11*, 995–1005.

Mitra, A., Flynn, K. J., Tillmann, U., Raven, J. A., Caron, D., Stoecker, D. K., Not, F., Hansen, P. J., Hallegraeff, G., Sanders, R., Wilken, S., McManus, G., Johnson, M., Pitta, P., Våge, S., Berge, T., Calbet, A., Thingstad, F., Jeong, H. J., … Lundgren, V. (2016). Defining planktonic protist functional groups on mechanisms for energy and nutrient acquisition: Incorporation of diverse mixotrophic strategies. *Protist*, *167*, 106–120.

Moeller, H. V., Neubert, M. G., & Johnson, M. D. (2019). Intraguild predation enables coexistence of competing phytoplankton in a well-mixed water column. *Ecology*, *100*(12), e02874. https://doi.org/10.1002/ecy.2874

O'Donnell, D. R., Hamman, C. R., Johnson, E. C., Kremer, C. T., Klausmeier, C. A., & Litchman, E. (2018). Rapid thermal adaptation in a marine diatom reveals constraints and trade-offs. *Global Change Biology*, *24*, 4554–4565.

Padfield, D., Yvon-Durocher, G., Buckling, A., Jennings, S., & Yvon-Durocher, G. (2016). Rapid evolution of metabolic traits explains thermal adaptation in phytoplankton. *Ecology Letters*, *19*, 133–142.

Patro, R., Duggal, G., Love, M. I., Irizarry, R. A., & Kingsford, C. (2017). Salmon provides fast and bias-aware quantification of transcript expression. *Nature Methods*, *14*, 417–419.

Polovina, J. J., Howell, E. A., & Abecassis, M. (2008). Ocean's least productive waters are expanding. *Geophysical Research Letters*, *35*(3), L03618.

Princiotta, S. D., Smith, B. T., & Sanders, R. W. (2016). Temperature-dependent phagotrophy and phototrophy in a mixotrophic chrysophyte. *Journal of Phycology*, *52*, 432–440.

R Core Team. (2020). *R: A language and environment for statistical computing*. R Foundation for Statistical Computing. https://R-project.org/

Rose, J. M., & Caron, D. A. (2007). Does low temperature constrain the growth rates of heterotrophic protists? Evidence and implications for algal blooms in cold waters. *Limnology and Oceanography*, *52*, 886–895.

Schaum, C. E., & Collins, S. (2014). Plasticity predicts evolution in a marine alga. *Proceedings of the Royal Society B: Biological Sciences*, *281*, 20141486.

Schaum, C.-E., Buckling, A., Smirnoff, N., Studholme, D. J., & Yvon-Durocher, G. (2018). Environmental fluctuations accelerate molecular evolution of thermal tolerance in a marine diatom. *Nature Communications*, *9*, 1719.

Simão, F. A., Waterhouse, R. M., Ioannidis, P., Kriventseva, E. V., & Zdobnov, E. M. (2015). BUSCO: Assessing genome assembly and annotation completeness with single-copy orthologs. *Bioinformatics*, *31*, 3210–3212.

Snell-Rood, E. C., Van Dyken, J. D., Cruickshank, T., Wade, M. J., & Moczek, A. P. (2010). Toward a population genetic framework of developmental evolution: The costs, limits, and consequences of phenotypic plasticity. *BioEssays*, *32*, 71–81.

Staehr, P. A., & Birkeland, M. J. (2006). Temperature acclimation of growth, photosynthesis and respiration in two mesophilic phytoplankton species. *Phycologia*, *45*, 648–656.

Stoecker, D. K. (1998). Conceptual models of mixotrophy in planktonic protists and some ecological and evolutionary implications. *European Journal of Protistology*, *34*, 281–290.

Thomas, M. K., Aranguren-Gassis, M., Kremer, C. T., Gould, M. R., Anderson, K., Klausmeier, C. A., & Litchman, E. (2017). Temperature–nutrient interactions exacerbate sensitivity to warming in phytoplankton. *Global Change Biology*, *23*, 3269–3280.

Thomas, M. K., Kremer, C. T., Klausmeier, C. A., & Litchman, E. (2012). A global pattern of thermal adaptation in marine phytoplankton. *Science*, *338*, 1085–1088.

Thornton, D. C. O. (2014). Dissolved organic matter (DOM) release by phytoplankton in the contemporary and future ocean. *European Journal of Phycology*, *49*, 20–46.

Trimborn, S., Thoms, S., Petrou, K., Kranz, S. A., & Rost, B. (2014). Photophysiological responses of Southern Ocean phytoplankton to changes in CO_2 concentrations: Short-term versus acclimation effects. *Journal of Experimental Marine Biology and Ecology*, *11*, 44–54.

Wahl, L. M., Gerrish, P. J., & Saika-Voivod, I. (2002). Evaluating the impact of population bottlenecks in experimental evolution. *Genetics*, *162*, 961–971.

Ward, B. A., & Follows, M. J. (2016). Marine mixotrophy increases trophic transfer efficiency, mean organism size, and vertical carbon flux. *Proceedings of the National Academy of Sciences of the United States of America*, *113*, 2958–2963.

West-Eberhard, M. J. (2003). *Developmental plasticity and evolution*. Oxford University Press.

Whitlock, M. C. (1996). The red queen beats the Jack-of-all-trades: The limitations on the evolution of phenotypic plasticity and niche breadth. *The American Naturalist*, *148*, S65–S77.

Wilken, S., Choi, C. J., & Worden, A. Z. (2020). Contrasting mixotrophic lifestyles reveal different ecological niches in two closely related marine protists. *Journal of Phycology*, *56*, 52–67.

Wilken, S., Huisman, J., Naus-Wiezer, S., & Van Donk, E. (2013). Mixotrophic organisms become more heterotrophic with rising temperature. *Ecology Letters*, *16*, 225–233.

Worden, A. Z., Follows, M. J., Giovannoni, S. J., Wilken, S., Zimmerman, A. E., & Keeling, P. J. (2015). Rethinking the marine carbon cycle: Factoring in the multifarious lifestyles of microbes. *Science*, *347*, 1257594.

Ying, B.-W., Matsumoto, Y., Kitahara, K., Suzuki, S., Ono, N., Furusawa, C., Kishimoto, T., & Yomo, T. (2015). Bacterial transcriptome reorganization in thermal adaptive evolution. *BMC Genomics*, *16*, 802.

Zhu, A., Ibrahim, J. G., & Love, M. I. (2019). Heavy-tailed prior distributions for sequence count data: Removing the noise and preserving large differences. *Bioinformatics*, *35*, 2084–2092.

Zubkov, M. V., & Tarran, G. A. (2008). High bacterivory by the smallest phytoplankton in the North Atlantic Ocean. *Nature*, *455*, 224–226.

SUPPORTING INFORMATION

Additional supporting information can be found online in the Supporting Information section at the end of this article.

How to cite this article: Lepori-Bui, M., Paight, C., Eberhard, E., Mertz, C. M., & Moeller, H. V. (2022). Evidence for evolutionary adaptation of mixotrophic nanoflagellates to warmer temperatures. *Global Change Biology*, *28*, 7094–7107. https://doi.org/10.1111/gcb.16431